

Characterization and Oxidative Addition Reactions of Different Rhodium and Iridium Triazolato Complexes

Alfred J. Muller, Jeanet Conradie*, Walter Purcell*, Stephen S. Basson and Johan A. Venter

Department of Chemistry, University of the Free State, Bloemfontein 9300, South Africa.

Received 17 June 2009, revised 7 December 2009, accepted 20 January 2010.

ABSTRACT

A number of different rhodium(I) and iridium(I) triazolato complexes and their oxidative addition products (triazolate = 3,5-bis(pyridine-2-yl)-1,2,4-triazolate (bpt⁻) and 4-amino-3,5-bis(pyridine-2-yl)-1,2,4-triazolate (bpt-NH⁻)) were prepared and characterized by means of IR and ¹H NMR spectroscopy, elemental analysis and computational chemistry methods. The oxidative addition reactions of these complexes with iodomethane in different solvents indicated simple second-order kinetics with the faster reactions in the more polar solvents ($1.44(7) \times 10^{-2} \text{ L mol}^{-1} \text{ s}^{-1}$ in dichloromethane compared with $9.2(5) \times 10^{-4} \text{ L mol}^{-1} \text{ s}^{-1}$ in benzene for iridium bpt-NH). ¹H NMR data and density functional theory calculations illustrate that the coordination of the metal centre in [M(bpt-NH)(cod)] (M = Rh or Ir) occurs *via* the amine moiety and a nitrogen of a pyridine ring.

KEY WORDS

Rhodium(I), iridium(I), triazole, cyclooctadiene, oxidative addition, methyl iodide, DFT.

1. Introduction

Rhodium and iridium remain the catalysts of choice when it comes to the production of acetic acid from methanol and account for over 60 % of the total acetic acid production worldwide. The first major process in the carbonylation of methanol was developed by Monsanto in the 1970s¹. This process, which used [Rh(I)₂(CO)₂]⁻ as catalyst, was purchased in 1986 by BP Chemicals who further developed the technology. In 1996 BP Chemicals announced a new advanced technology, called the Cativa process, which replaced the rhodium catalyst with an iridium catalyst, in conjunction with novel promoters such as rhenium, ruthenium and osmium. Benefits achieved with the change in catalyst include cheaper iridium prices, a faster and more effective process, less catalyst required, larger turnover numbers and fewer side products.² In the 1980s Celanese announced an improved Monsanto process (OA Plus) which succeeded in increasing the rhodium catalyst stability by the addition of high concentrations of lithium iodide, which reduced the water concentrations and improved the carbonylation rate. The market share of these two companies is currently 25 % each and they are engaged in a battle for global leadership.

Other methods for the production of acetic acid include the aerobic fermentation of ethanol which is still being used by Perkebunan Nusantra in Indonesia, the liquid phase oxidation of acetaldehyde in the presence of Mn(OAc)₂ or Co(OAc)₂, the oxidation of *n*-butane and light naphtha in the presence of cobalt or manganese, the Chiyoda Acetica process, which makes use of heterogeneous supported catalysis, the direct oxidation of ethylene in the vapour phase, selective ethane oxidation in the presence of molybdenum, vanadium and niobium and finally coal-based technology, which converts methyl acetate to acetic anhydride.³

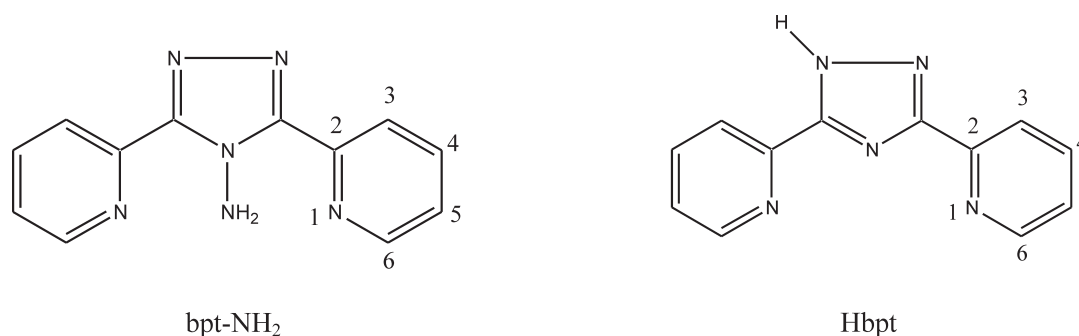
Research has shown that the actual catalytic cycles of the Monsanto and Cativa⁴ processes consist of a series of reactions including oxidative addition, 1,1-insertion or CO insertion, CO association and reductive elimination.⁵⁻⁷ All these reactions were

studied in detail by a large number of researchers, involving numerous rhodium and iridium complexes. These involved structural and mechanistic studies in which researchers manipulated, for example, the nucleophilicity of the metal centre using different mono- and bidentate ligands or changing the steric bulk within the complex to change the rates of the different key reactions in the process.⁸ An example of this continued study is that done by Kurmari *et al.*, in which they studied, for example, the influence of different phosphines^{9,10} and pyridine aldehyde ligands^{11,12} on the oxidative addition of Rh(I) complexes.

Numerous structural and kinetic studies were also undertaken in our laboratory to determine the factors that influence the nucleophilicity of the metal centres, involving both iridium and rhodium. Many of these studies included *p*-block donor atoms such as carbon (cyclo-octadiene), phosphorus (PX₃ and POX₃), arsine (AsPh₃) and stibine (SbPh₃) as well as combinations of these atoms. The studies also included the utilization of different monocharged bidentate ligands such as acetylacetonato, hexafluoroacetylacetonato, methoxy-*N*-methylbenzothiohydroximato, *N*-aryl-*N*-nitrosohydroxylamines and amino-vinylketones, which involved a change in the combination of donor atoms to determine their influences on the reactivity and mechanism of the metal complexes.¹³ Results obtained from these studies indicated that the *trans* influence of asymmetrical bidentate ligands with different donor atoms follows the reverse electronegativity order, i.e. S > N > O,¹⁴⁻¹⁶ while the donor atom combinations for the different bidentate ligands in [Rh(LL)(CO)(PPh₃)₂] complexes showed the following oxidative addition order N,S > N,O > S,O > O,O.¹⁷

Absent from the donor atom range is the N,N combination and it was decided to synthesize different rhodium and iridium complexes containing N,N bidentate ligands to investigate this combination on the rate of oxidative addition reactions. Two different ligands, namely 3,5-bis(pyridine-2-yl)-1,2,4-triazole (Hbpt), which allowed for the formation of five-membered chelates and 4-amino-3,5-bis(pyridine-2-yl)-1,2,4 triazole, (bpt-NH₂), which has the appropriate chemical geometry to behave

* To whom correspondence should be addressed.
E-mail addresses: purcellw@ufs.ac.za / conradj@ufs.ac.za.

Chemical structures of bpt-NH₂ and Hbpt

as an anionic or neutral bidentate chelating group (five- or six-membered), were synthesized. The oxidative addition between CH₃I and [M(cod)(L,L')]₂ (M = Rh and Ir; L,L' = bpt⁻ and bpt-NH) was then studied to determine the influence of these ligands on the rate of oxidative addition.

2. Experimental

2.1. General Considerations

All the preparations were performed in a dry nitrogen atmosphere and unless otherwise stated all chemicals were reagent grade and used without further purification. IR spectra were recorded with a Hitachi 270-50 spectrophotometer (Tokyo, Japan), while the NMR spectra were obtained at 293 K on a Bruker (Karlsruhe, Germany) 300 MHz spectrometer. The elemental analyses were done by the Canadian Micro Analytical Service, Delta, BC, Canada. The methyl iodide was stabilized by silver foil to prevent decomposition and used in a well-ventilated fume cupboard.

The UV/visible spectra and kinetic runs were performed on a Varian Cary-50 double-beam spectrophotometer (Palo Alto, CA, USA) in a thermostatically controlled holder (± 0.1 °C), which has a capacity of 18 cells. The solvents used for the kinetic runs were all purified and dried using prescribed methods.¹⁸ The metal complexes were freshly prepared before each reaction to minimize the extent of an observed solvolysis reaction ($t_{1/2} = 360$ min). Typical experimental conditions were [M(cod)(LL)] = 1.0×10^{-3} mol L⁻¹, and [CH₃I] varied between 0.017 and 0.17 mol L⁻¹, which ensured good pseudo-first-order plots of $\ln(A_t - A_\infty)$ vs. time for at least two half-lives, with A_t and A_∞ the absorbances at time t and infinity, respectively. The observed first-order rate constants were calculated from the above plots using a non-linear least squares program.¹⁹

2.2. Synthesis

2.2.1. 4-Amino-3,5-bis(pyridine-2-yl)-1,2,4-triazole (bpt-NH₂) and 3,5-bis(pyridine-2-yl)-1,2,4-triazole (Hbpt)

Both ligands were synthesized using a three-step process proposed by Geldard and Lions.²⁰

From the synthesis, 4-amino-3,5-bis(pyridine-2-yl)-1,2,4-triazole (bpt-NH₂) (76 %) was obtained as colourless needles: δ_{H} (300 MHz, CDCl₃): 8.68 (H6,1H,d), 8.55 (NH₂,2H,s), 8.42 (H3,1H,d), 7.91 (H4,1H,d,t), 7.40 ppm (H5,1H,d,d,d) (t = triplet, d = doublet, s = singlet). IR_{KBr}: $\nu(\text{NH})$, 3298, $\nu(\text{C}=\text{C})$, $\nu(\text{C}=\text{N})$, 1590, 1566, 1549, 1520 cm⁻¹.

From the synthesis, 3,5-bis(pyridine-2-yl)-1,2,4-triazole (Hbpt) (43 %) was obtained as colourless needles: δ_{H} (300 MHz, CDCl₃): 8.78 (H6,1H,d,d), 8.36 (H3,1H,d,d), 7.38 (H4,1H,t,d,d), 7.40 (H5,1H,d,d,d), 2.1 ppm (NH,1H,s). IR_{KBr}: $\nu(\text{C}=\text{C})$, $\nu(\text{C}=\text{N})$, 1593, 1575, 1509 cm⁻¹.

2.2.2. Bis-(η^4 -cyclo-octa-1,5-diene- μ -chloridoiridium(I) [Ir(Cl)(cod)]₂ and bis-(η^4 -cyclo-octa-1,5-diene- μ -chloridorhodium(I) [Rh(Cl)(cod)]₂)

The iridium dimer was synthesized according to the method proposed by Bezman *et al.*,²¹ while the rhodium analogue was synthesized according to Giordano and Crabtree.²²

From the synthesis, bis-(η^4 -cyclo-octa-1,5-diene- μ -chloridoiridium(I)) (81 %) was obtained as orange crystals: δ_{H} (300 MHz, CDCl₃): 4.22 (8H,s), 2.26 (8H,s), 1.53 ppm (8H,t). IR_{KBr}: $\nu(\text{C}=\text{C})$, 1476, 1449 cm⁻¹ (cod).

From the synthesis, bis-(η^4 -cyclo-octa-1,5-diene- μ -chloridorhodium(I)) (94 %) was obtained as yellow-orange crystals. δ_{H} (300 MHz, CDCl₃): 4.2 (8H,s), 2.48 (8H,s), 1.72 ppm (8H,t). IR_{KBr}: $\nu(\text{C}=\text{C})$, 1326, 993 cm⁻¹ (cod).

2.2.3. 3,5-Bis(pyridine-2-yl)-1,2,4-triazolato- η^4 -cyclo-octa-1,5-diene-iridium(I) [Ir(bpt)(cod)] (1)

KOH (0.0180 g, 0.03209 mmol) was dissolved in MeOH (3.2 mL) in a 100 mL two-neck round-bottom flask under a nitrogen atmosphere. 3,5-bis(pyridine-2-yl)-1,2,4-triazole (0.0665 g, 0.2978 mmol) was added to this KOMe solution and stirred until all the ligand had dissolved. [Ir(Cl)(cod)]₂ (0.1 g, 0.1489 mmol) was dissolved in deoxygenated dichloromethane (DCM, 4.3 mL) in a two-neck round-bottom flask while kept under a nitrogen atmosphere. The solution containing the deprotonated Hbpt was subsequently transferred with a syringe to the solution containing the iridium and the solvent was then removed with nitrogen gas. The red solid was re-dissolved in deoxygenated DCM and filtered through a fritted glass funnel packed with celite whilst maintaining a nitrogen atmosphere over the funnel. The solution was again removed with nitrogen and the final product was kept under a nitrogen atmosphere to prevent decomposition. From the synthesis, 3,5-bis(pyridine-2-yl)-1,2,4-triazolato- η^4 -cyclo-octa-1,5-diene-iridium(I) (67 %) was obtained as a red solid: δ_{H} (300 MHz, CDCl₃): (bpt) 8.7 (1H, d), 8.19 (2H,d,d), 7.97 (1H,t), 7.91 (1H,t), 7.72 (1H,t,d), 7.23 (1H,m), 7.19 ppm (1H,s). cod : δ 5.0 (2H,s), 4.64 (2H,s), 2.42 (4H,d,d), 1.88 ppm (4H,d,d). IR_{KBr}: $\nu(\text{C}=\text{C})$, 1635, 1476, 1449, 1428 cm⁻¹. Found: C, 45.61, N, 13.22, H, 3.80, Ir, 35.4 %. Calc. for C₂₀H₂₀N₅Ir (522.63); 45.97, N, 13.40, H, 3.86, Ir, 36.78 %.

2.2.4. 4-Amino-3,5-bis(pyridine-2-yl)-1,2,4-triazolato- η^4 -cyclo-octa-1,5-diene-iridium(I) [Ir(bpt-NH)(cod)] (2)

The preparation of the [Ir(bpt-NH)(cod)] complex was similar to that of [Ir(bpt)(cod)]. For this preparation, 0.0709 g (0.23 mmol) 4-amino-3,5-bis(pyridine-2-yl)-1,2,4-triazole was used as ligand while the rest of the chemicals were kept the same and an orange product was isolated. From the synthesis, 4-amino-3,5-bis(pyridine-2-yl)-1,2,4-triazolato- η^4 -cyclo-octa-1,5-diene-iridium(I) was obtained as an orange solid (58.6 %). δ_{H} (300 MHz, CDCl₃): (bpt-NH) 10.92 (NH,1H,s), 9.2 (1H,d,d), 8.68 (2H,d), 8.55 (1H,d), 8.50 (1H,s), 8.45 (1H,d,d), 8.15 (1H,d), 8.01 ppm (1H,t), cod: δ 4.17

(2H,s), 3.4 (2H,s), 2.4 (4H,d), 1.92 ppm (4H, d). IR_{KBr}: $\nu(\text{C}=\text{C})$, 1620, 1593, 1566 cm^{-1} . Found: C, 45.97, N, 15.54, H, 3.91, Ir, 34.01 %. Calc. for $\text{C}_{20}\text{H}_{21}\text{N}_6\text{Ir}$ (537.63); C, 44.68, N, 15.63, H, 3.94, Ir, 35.75 %.

2.2.5. 3,5-Bis(pyridine-2-yl)-1,2,4-triazolato- η^4 -cyclo-octa-1,5-diene-rhodium(I) [Rh(bpt)(cod)] (3)

The preparation of the [Rh(bpt-NH)(cod)] complex was basically the same as the above-mentioned procedure. For this preparation, 0.0665 g (0.2978 mmol) 4-amino-3,5-bis(pyridine-2-yl)-1,2,4-triazole and 0.075 g (0.1527 mmol) [Rh(cod)Cl]₂ was used. The reaction mixture containing the deprotonated ligand as well as the metal complex was stirred for 3 h, after which diethyl ether was added to precipitate the orange product. Recrystallization was performed in the same fashion as above. From the synthesis, 3,5-bis(pyridine-2-yl)-1,2,4-triazolato- η^4 -cyclo-octa-1,5-diene-rhodium(I) (74.4 %) was obtained as an orange solid. δ_{H} (300 MHz, CDCl₃): (bpt⁻) 8.7 (1H,s), 8.23 (2H,d), 7.9 (1H,s), 7.79 (1H,s), 7.65 (1H,s), 7.32 (1H,s), 7.25 ppm (1H,s), cod: δ 4.64 (4H,s), 2.58 (2H,s), 2.32 (2H,s), 2.08 ppm (4H,t). IR_{KBr}: $\nu(\text{C}=\text{C})$, 1614, 1593, 1569, 1530 cm^{-1} . Found: C, 55.22, N, 16.05, H, 4.57, Rh, 22.9 %. Calc. for $\text{C}_{20}\text{H}_{20}\text{N}_5\text{Rh}$ (433.33); C, 55.44, N, 16.16, H, 4.65, Rh, 23.75 %.

2.2.6. 4-Amino-3,5-bis(pyridine-2-yl)-1,2,4-triazolato- η^4 -cyclo-octa-1,5-diene-rhodium(I) [Rh(bpt-NH)(cod)] (4)

The same procedure was used as above. From the synthesis, 4-amino-3,5-bis(pyridine-2-yl)-1,2,4-triazolato- η^4 -cyclo-octa-1,5-diene-rhodium(I) (68.2 %) was isolated as an orange solid. δ_{H} (300 MHz, CDCl₃): (bpt-NH) NH 9.16 (1H,s), 8.9 (1H,s), 8.70 (2H,s), 8.49 (2H,s), 8.38 (2H,s), 7.4 ppm (1H, s), cod: δ 4.35 (2H,s), 2.5 (4H,s), 2.55 (4H,s), 2.38 ppm (2H,s). IR_{KBr}: $\nu(\text{C}=\text{C})$, 1620, 1593, 1566 cm^{-1} . Found: C, 52.98, N, 18.25, H, 4.61, Rh, 21.80 %. Calc. for $\text{C}_{20}\text{H}_{21}\text{N}_6\text{Rh}$ (448.34); C, 53.58, N, 18.75, H, 4.72, Rh, 22.95 %.

2.2.7. Iodido-3,5-bis(pyridine-2-yl)-1,2,4-triazolato-methyl- η^4 -cyclo-octa-1,5-diene-iridium(I) [Ir(bpt)(cod)(CH₃)I] (5)

[Ir(cod)(bpt)] (0.015 g, 0.026 mmol) was dissolved in deoxygenated acetone (10 mL) and heated on a water bath to 30 °C. An excess of CH₃I (2.6 mmol) was added to this solution and the mixture was stirred for 30 min, while the volume of the acetone was kept constant by the periodic addition of the solvent. Diethyl ether was added to precipitate the product and the mixture was centrifuged. The yellow solid was dried overnight in a vacuum desiccator over P₂O₅. From the synthesis, iodido-3,5-bis(pyridine-2-yl)-1,2,4-triazolato-methyl- η^4 -cyclo-octa-1,5-diene-iridium(I) (72 %) was isolated as a yellow solid. δ_{H} (300 MHz, CDCl₃): (bpt⁻) 8.68 (1H,d), 8.40 (2H,d,d), 8.15 (1H,d), 7.85 (1H,t), 7.72 (1H,t,d), 7.34 (1H,m), 7.19 ppm (1H,s), cod: δ 3.80 (2H,s), 3.32 (2H,s), 2.65 (4H,d,d), 1.80 ppm (CH₃,3H,s). IR_{KBr}: $\nu(\text{C}=\text{C})$, 1620, 1500 cm^{-1} . Found: C, 37.8, N, 10.44, H, 3.42, Ir, 26.88, I, 18.3 %. Calc. for $\text{C}_{21}\text{H}_{23}\text{N}_5\text{IrI}$ (664.58); C, 37.95, N, 10.54, H, 3.49, Ir, 28.92, I, 19.10 %.

2.2.8. Iodido-4-amino-3,5-bis(pyridine-2-yl)-1,2,4-triazolato-methyl- η^4 -cyclo-octa-1,5-diene-iridium(I), [Ir(bpt-NH)(cod)(CH₃)I] (6)

The same procedure was used as above. From the synthesis, iodido-4-amino-3,5-bis(pyridine-2-yl)-1,2,4-triazolato-methyl- η^4 -cyclo-octa-1,5-diene-iridium(I) (54 %) was isolated as a yellow solid. δ_{H} (300 MHz, CDCl₃): (bpt-NH⁻) 8.88 (NH,1H,s), 8.68 (1H,d,d), 8.38 (2H,d), 8.10 (1H,d), 7.98 (1H,s), 7.88 (1H,d,d), 7.38 (1H,d), 7.25 ppm (1H,t), cod: δ 3.35 (2H,s), 2.95 (2H,s), 2.82 (4H,d), 2.09 (4H,d), 1.78 ppm (CH₃,3H,s). IR_{KBr}: $\nu(\text{C}=\text{C})$, 1620, 1593 cm^{-1} . Found: C, 36.74, N, 12.09, H, 3.41, Ir, 27.5, I, 17.16 %.

Calc. for $\text{C}_{21}\text{H}_{24}\text{N}_6\text{IrI}$ (679.59); C, 37.12, N, 12.36, H, 3.56, Ir, 28.28, I, 18.67 %.

2.2.9. Iodido-3,5-bis(pyridine-2-yl)-1,2,4-triazolato-methyl- η^4 -cyclo-octa-1,5-diene-rhodium(I) [Rh(bpt)(cod)(CH₃)I] (7)

The same procedure was used as above. From the synthesis, iodido-3,5-bis(pyridine-2-yl)-1,2,4-triazolato-methyl- η^4 -cyclo-octa-1,5-diene-rhodium(I) (80 %) was isolated as a yellow-orange solid. δ_{H} (300 MHz, CDCl₃): 8.75 (1H,s), 8.08 (2H,d), 7.88 (1H,s), 7.75 (1H,s), 7.58 (1H,s), 7.48 (1H,s), 7.25 ppm (1H,s), cod: δ 4.68 (4H,s), 2.93 (4H,s), 2.35 (2H,s), 2.08 (4H,t), 1.70 ppm (CH₃,3H,s). IR_{KBr}: $\nu(\text{C}=\text{C})$, 1614, 1497 cm^{-1} . Found: C, 43.67, N, 12.12, H, 3.99, Rh, 17.1, I, 21.60 %. Calc. for $\text{C}_{20}\text{H}_{20}\text{N}_5\text{RhI}$ (574.58); C, 43.90, N, 12.19, H, 4.03, Rh, 17.91, I, 22.09 %.

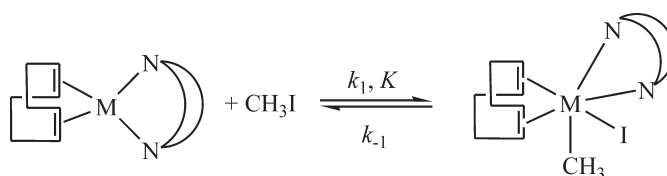
2.2.10. Iodido-4-amino-3,5-bis(pyridine-2-yl)-1,2,4-triazolato-methyl- η^4 -cyclo-octa-1,5-diene-rhodium(I), [Rh(bpt-NH)(cod)(CH₃)I] (8)

The same procedure was used as above. From the synthesis, iodido-4-amino-3,5-bis(pyridine-2-yl)-1,2,4-triazolato-methyl- η^4 -cyclo-octa-1,5-diene-rhodium(I) (90 %) was isolated as a yellow solid. δ_{H} (300 MHz, CDCl₃): 8.95 (NH,1H,s), 8.75 (1H,s), 8.55 (2H,s), 8.35 (2H,s), 7.95 (2H,s), 7.25 ppm (1H,s), cod: δ 4.58 (2H,s), 2.92 (2H,s), 2.65 (4H,s), 2.14 (CH₃,3H,s), 2.08 ppm (4H,s). IR_{KBr}: $\nu(\text{C}=\text{C})$, 1437 cm^{-1} . Found: C, 42.10, N, 14.16, H, 4.01, Rh, 16.9, I, 10.90 %. Calc. for $\text{C}_{21}\text{H}_{24}\text{N}_6\text{RhI}$ (590.23); C, 42.73, N, 14.24, H, 4.10, Rh, 17.43, I, 10.50 %.

2.3. Kinetics

The UV/visible spectra of the oxidative addition reactions between the metal complex and methyl iodide showed only one reaction. This was the case for all the different rhodium and iridium complexes that were studied. Variations of methyl iodide concentrations indicated a linear relationship with an intercept close to zero (see Fig. 1).

These results led to a very simple reaction mechanism



with M = Ir(I) or Rh(I).

The rate law for this reversible reaction is given by Equation 1

$$R = k_1[\text{M}(\text{LL})(\text{cod})][\text{CH}_3\text{I}] - k_{-1}[\text{M}(\text{LL})(\text{cod})(\text{CH}_3)\text{I}] \quad (1)$$

The observed rate constant, after integration and using pseudo-first-order conditions, is given by Equation 2

$$k_{\text{obs}} = k_1[\text{CH}_3\text{I}] + k_{-1} \quad (2)$$

The values for k_1 and k_{-1} were calculated from plots of k_{obs} vs. [CH₃I] for the different complexes in different solvents and are reported in Table 1. These calculations indicated that the k_{-1} values for the different complexes are all zero within experimental error.

2.4. Computational Methods

The DFT studies were carried out using the OLYP²³ and the B3LYP²⁴ functionals, ZORA-TZP basis set,²⁵ fine grids for numerical integration of matrix elements, tight SCF and geometry optimization criteria, and a spin-restricted formalism, all as implemented in the ADF 2009 program system.²⁶ All calculations were performed in the gas phase.

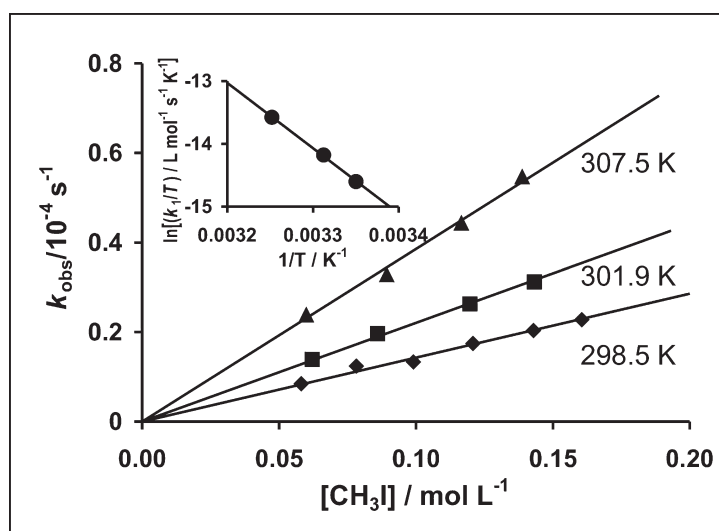


Fig. 1 k_{obs} vs. $[\text{CH}_3\text{I}]$ for the oxidative addition reaction of $[\text{Rh}(\text{bpt})(\text{cod})]$ and CH_3I in acetone at different temperatures. Inset: linear dependence between $\ln(k_f/T)$ and $1/T$, as predicted by the Eyring equation.

3. Discussion

3.1. Synthesis of Complexes

The three new metal(I) complexes, $[\text{Ir}(\text{bpt})(\text{cod})]$ (1), $[\text{Ir}(\text{bpt-NH})(\text{cod})]$ (2), $[\text{Rh}(\text{bpt})(\text{cod})]$ (3), and one known²⁷ complex $[\text{Rh}(\text{bpt-NH})(\text{cod})]$ (4), were obtained by reacting the deprotonated bpt or bpt-NH ligands with $[\text{M}(\text{Cl})(\text{cod})]_2$, $\text{M} = \text{Ir}$ or Rh , under an inert atmosphere. The metal(I) complexes 1–4 were well characterized by their IR and NMR spectra. Elemental analyses show an excellent correlation between the experimental and calculated percentages of the different complexes. The nitrogen and metal percentages, as well as the nitrogen to metal ratios, are in agreement with those expected for the different complexes, viz. a 5:1 N:metal ratio for the bpt complexes, while a 6:1 N:metal ratio was obtained for the bpt-NH complexes. In the case of the bpt-NH ligand, the metal centre may be coordinated either *via* the amido moiety and the pyridine ring, resulting in the formation of a six-membered anionic ring structure, or *via*

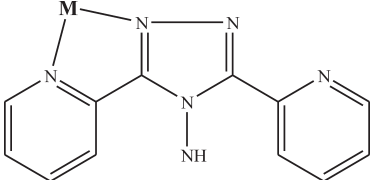
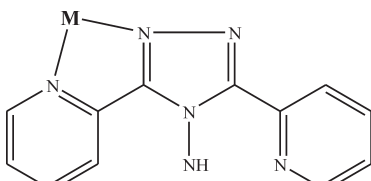
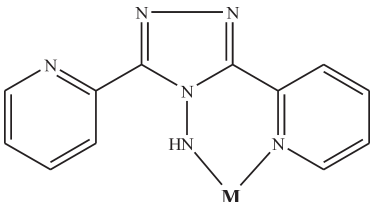
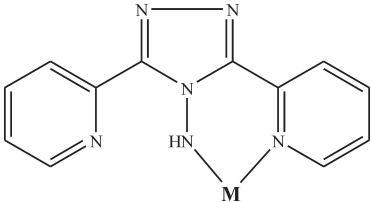
the triazole ring and the pyridine ring, resulting in the formation of a five-membered ring structure. Furthermore, the uncoordinated pyridine ring may adopt different orientations (see Table 2 first column). The coordination mode of the bpt-NH ligand could not be determined with certainty at this stage from the physical data that were collected. However, DFT calculations indicated that a six-membered ring structure seems the most likely for this ligand.

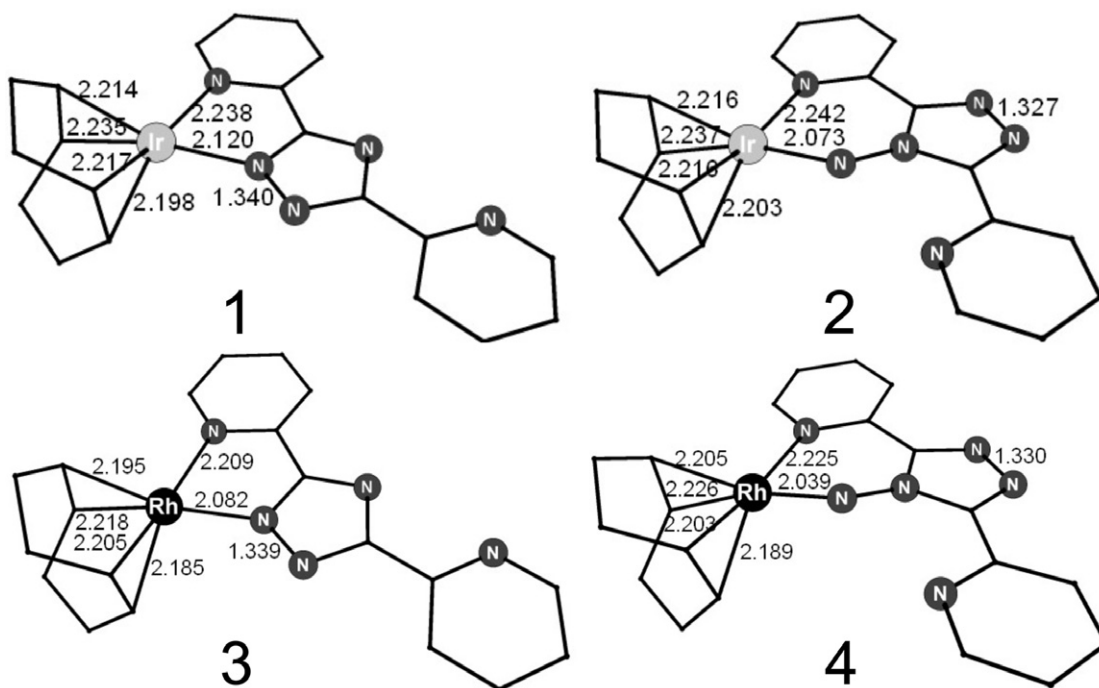
The difference between these two coordination modes can be deduced from a ^1H NMR perspective. The formation of the six-membered ring structure should give rise to a significant downfield shift of the singlet associated with the amide moiety with respect to the free ligand. The singlet associated with the NH moiety was found at δ 10.92 and 9.16 ppm for $[\text{Ir}(\text{bpt-NH})(\text{cod})]$ (2) and $[\text{Rh}(\text{bpt-NH})(\text{cod})]$ (4), respectively, whereas that of the free ligand was observed at δ 8.55 ppm. The ^1H NMR shift observed for the six-membered $[\text{Rh}(\text{bpt-NH})(\text{cod})]$ complex of this study (δ 9.16 ppm in CDCl_3), is in agreement with

Table 1 Summary of the kinetic data for the oxidative addition reactions between $[\text{M}(\text{LL})(\text{cod})]$ and CH_3I ($\text{M} = \text{Rh}(\text{I})$ and $\text{Ir}(\text{I})$, $\text{LL} = \text{bpt}$ and bpt-NH) in different solvents and at different temperatures.

Complex	Solvent	Temperature/K	$k_f/10^{-2} \text{ L mol}^{-1} \text{ s}^{-1}$	$k_{-f}/10^{-4} \text{ s}^{-1}$	$\Delta H^\ddagger/\text{kJ mol}^{-1}$	$\Delta S^\ddagger/\text{J K}^{-1} \text{ mol}^{-1}$
$[\text{Ir}(\text{bpt})(\text{cod})]$	acetone (500 nm)	288.9	0.141(6)	1.8(5)	42.8(6)	-150(2)
		302.5	0.35(1)	0.4(1)		
		311.3	0.58(2)	0.3(1)		
$[\text{Ir}(\text{bpt-NH})(\text{cod})]$	benzene (340 nm)	287.9	0.044(2)	0.02(2)	42(2)	-162(8)
		297.8	0.092(5)	0.03 (6)		
		310.6	0.184(3)	0.15(3)		
$[\text{Ir}(\text{bpt-NH})(\text{cod})]$	DCM (400 nm)	288.7	1.00(5)	0.2(5)	46(12)	-123(22)
		297.9	1.44(7)	1.1(8)		
		304.1	2.5(2)	-1(2)		
$[\text{Rh}(\text{bpt})(\text{cod})]$	acetone (500 nm)	298.5	0.0136(8)	0.008(9)	40(8)	-131(6)
		301.9	0.021(2)	0.01(2)		
		307.5	0.039(3)	-0.01(5)		
$[\text{Rh}(\text{bpt-NH})(\text{cod})]$	benzene (412 nm)	288.5	0.114(3)	1.3(3)	51(2)	-124(7)
		297.5	0.21(2)	0.01(2)		
		307.7	0.429(6)	-0.01(5)		
$[\text{Rh}(\text{bpt-NH})(\text{cod})]$	DCM (420 nm)	288.9	1.23(3)	1.3(3)	37(4)	-152(14)
		297.9	2.20(3)	0.4(3)		
		303.9	2.9(1)	2(2)		

Table 2 DFT molecular energies of the possible coordination modes and stereo isomers of [M(bpt-NH)(cod)], M = Ir (2) or Rh (4) relative to the lowest energy isomer in each case.

Geometry	Five- or six-membered ring	Energy/kJ mol ⁻¹	
		Ir	Rh
	5	50.1	37.0
	5	23.8	19.7
	6	72.3	41.1
	6	0.0	0.0

**Figure 2** The DFT-calculated minimum energy geometries of [Ir(bpt)(cod)] (1), [Ir(bpt-NH)(cod)] (2), [Rh(bpt)(cod)] (3) and [Rh(bpt-NH)(cod)] (4). Selected bond lengths (Å) are as indicated. H atoms omitted for clarity.

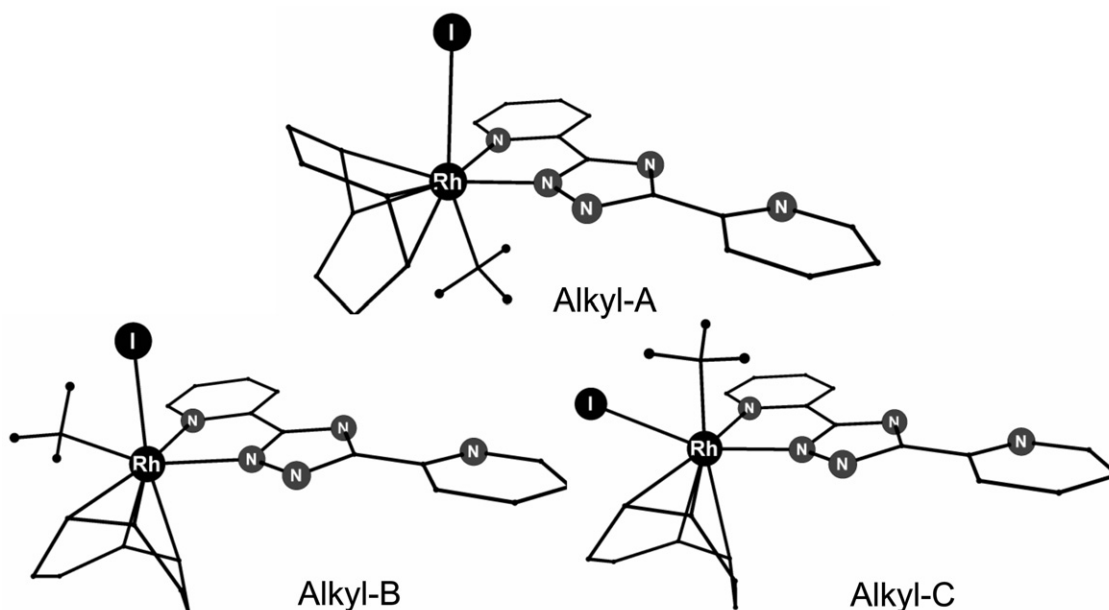


Figure 3 The DFT-calculated minimum energy geometries showing the stereo arrangement of the three different alkyl product isomers of the oxidative addition of CH_3I to $[\text{Rh}(\text{bpt})(\text{cod})]$ (7): alkyl-A (top, *trans* addition), alkyl-B (bottom left, *cis1* addition) and alkyl-C (bottom right, *cis2* addition). H atoms omitted for clarity, except for the methyl hydrogens.

the singlet associated with the NH moiety of six-membered $[\text{Rh}(\text{phen})_2(\text{bpt-NH})]^{2+}$ and six-membered $[\text{Rh}(\text{bpy})_2(\text{bpt-NH})]^{2+}$ (δ 9.11 and 9.16 ppm respectively in DMSO-d_6) relative to that of the free ligand at δ 7.82 ppm in DMSO-d_6 . However, the singlet associated with the NH moiety of the five-membered $[\text{Rh}(\text{bpt-NH})(\text{cod})]^+$ and the related five-membered $[\text{Rh}(\text{bpy})_2(\text{bpt-NH}_2)]^{3+}$ complexes were found at δ 8.51 (acetone- d_6)²⁷ and 7.66 ppm (DMSO-d_6),²⁸ which is comparable with that of the free ligand (δ 8.76 ppm in acetone- d_6 and 7.82 ppm in DMSO-d_6). No NMR data of the previously synthesized six-membered $[\text{Rh}(\text{bpt-NH})(\text{cod})]$ (4) complex are available, but the reported IR data²⁷ are in agreement with the IR data of this study.

In a further investigation of the unknown structure of $[\text{Ir}(\text{bpt-NH})(\text{cod})]$ (2) and $[\text{Rh}(\text{bpt-NH})(\text{cod})]$ (4) density functional theory calculations on the possible isomers of the two coordination modes of the bpt-NH^- to rhodium(I) and iridium(I) in 2 and 4 were performed. Calculations also showed that the six-membered ring complexes with the nitrogen of the uncoordinated pyridine ring rotated in the same direction as the amine moiety, to be more stable by 23.8–72.3 kJ mol^{-1} (see Table 2). The minimum energy optimized structures of 1–4 are presented in Fig. 2 with selected bond lengths shown.

Oxidative addition of CH_3I to 1–4 leads to alkyl products, $[\text{Ir}(\text{bpt})(\text{cod})(\text{CH}_3)\text{I}]$ (5), $[\text{Ir}(\text{bpt-NH})(\text{cod})(\text{CH}_3)\text{I}]$ (6), $[\text{Rh}(\text{bpt})(\text{cod})(\text{CH}_3)\text{I}]$ (7) or $[\text{Rh}(\text{bpt-NH})(\text{cod})(\text{CH}_3)\text{I}]$ (8), respectively. Three possible metal(III) alkyl isomers of each complex are possible: one (alkyl-A) if *trans* addition occurs and two possible isomers (alkyl-B and alkyl-C) if *cis* addition occurs (see Fig. 3 for the isomers of 7). Complexes 5–8 were isolated successfully. Elemental analyses confirmed the presence of I and CH_3 in the

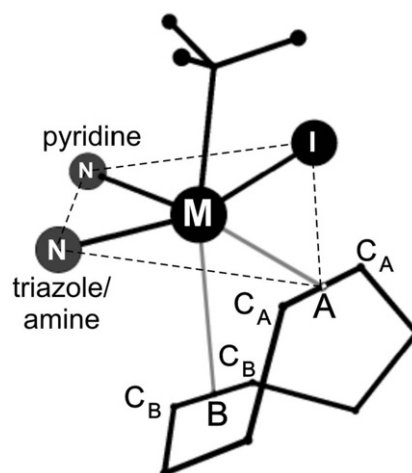


Figure 4 Basic structural view of the octahedral metal(III) complexes 5–8 showing the coordination sphere around the metal. M = Ir or Rh, A and B are the centroids of the two double bonds of the coordinated cod ligand. The methyl group and B are above and below the square plane.

isolated metal complexes. The ^1H NMR signal of the CH_3 group, between δ 1.5 and 2.7 ppm is a typical chemical shift of a CH_3 group attached to rhodium(III)²⁹ or iridium(III).⁴⁸ Knowledge of the stereochemistry of the reaction products may contribute to the rationalization of experimental results and furnish ideas which might be used to design new and better ligands. A DFT study on the ground state molecular structures of three possible alkyl product isomers of each of 5–8 shows that the *cis* addition product, alkyl-C is the most stable (see Table 3). The geometry of

Table 3 DFT molecular energies (kJ mol^{-1}) of the possible alkyl reaction products of the oxidative addition reaction of 1–4 and CH_3I relative to the alkyl-C isomer in each case.

	Geometry	$[\text{Ir}(\text{bpt})(\text{cod})-(\text{CH}_3)\text{I}]$ (5)	$[\text{Ir}(\text{bpt-NH})(\text{cod})-(\text{CH}_3)\text{I}]$ (6)	$[\text{Rh}(\text{bpt})(\text{cod})-(\text{CH}_3)\text{I}]$ (7)	$[\text{Rh}(\text{bpt-NH})(\text{cod})-(\text{CH}_3)\text{I}]$ (8)
alkyl-A	<i>trans</i>	18.0	20.1	25.2	28.8
alkyl-B	<i>cis1</i>	20.9	37.6	30.6	55.3
alkyl-C	<i>cis2</i>	0.0	0.0	0.0	0.0

Table 4 DFT/B3LYP calculated (complexes 5–8) and experimental bond distances and angles for different Ir(III) and Rh(III) complexes.

Complex	Ring size	Bond length/Å								Angle/°				Ref		
		M-I	M-C _{CH3}	M-C _{cod A}	M-C _{cod B}	M-C _{cod A}	M-C _{cod B}	M-C _{cod B}	M-N _{pyridine}	M-N _{nitrato/pyridine}	N _{nitrato/pyridine} -M-A _{cod}	C _{CH3} -M-I	C _{CH3} -M-B _{cod}		C _{CH3} -M-A _{cod}	
[Ir(bpt)(cod)(CH ₃)I], 5	5	2.886	2.129	2.335	2.310	2.603	2.640	2.225	2.150	76.0	99.8	82.9	171.6	93.7	calc	this study
[Ir(bpt-NH)(cod)(CH ₃)I], 6	6	2.937	2.122	2.321	2.282	2.719	2.244	2.244	2.168	80.8	95.9	84.0	168.8	91.3	calc	this study
[Rh(bpt)(cod)(CH ₃)I], 7	5	2.862	2.100	2.371	2.335	2.648	2.694	2.189	2.115	76.9	99.5	83.4	151.7	94.6	calc	this study
[Rh(bpt-NH)(cod)(CH ₃)I], 8	6	2.921	2.089	2.370	2.317	2.823	2.693	2.205	2.125	81.7	95.4	84.2	167.7	92.0	calc	this study
[Ir(COD)(m-Cl)(SnCl ₃)Cl] ₂	4	2.385	2.185	2.222	2.221	2.222	2.222	2.222	80.9	71.2	90.1	173.2	90.1	173.2	exp	32a
[Rh(COD)(m-Cl)(SnCl ₃)Cl] ₂	4	2.392	2.177	2.230	2.227	2.227	2.202	2.202	82.9	65.7	90.7	171.6	90.7	171.6	exp	32b
[Ir(COD)(m-Cl)(SnCl ₂ CH ₃)Cl] ₂	4	2.371	2.171	2.168	2.177	2.177	2.197	2.197	80.7	71.6	90.1	173.8	90.1	173.8	exp	32b
[Rh(neocupf)(CO)(PPh ₃)(CH ₃)I]	5	2.711	2.092	2.143	2.160	2.178	2.190	2.050	76.3	91.2	90.8	176.6	91.2	176.6	exp	34
[Rh(cupf)(CO)(PPh ₃)(CH ₃)I]	5	2.708	2.081	2.166	2.153	2.175	2.143	2.076	74.9	90.8	90.8	175.8	90.8	175.8	exp	13c
[Rh(fctfa)(CO)(PPh ₃)(CH ₃)I]	6	2.716	2.077	2.161	2.166	2.175	2.143	2.076	88.1	87.3	87.3	177.7	87.3	177.7	exp	13m
[Ir(acac)(cod)(CH ₃)I]	6	2.833	2.168	2.143	2.160	2.178	2.190	2.050	M-O/S	O-M/O/S	O-M/O/S	C _{CH3} -M-I	C _{CH3} -M-I	C _{CH3} -M-I	exp	30
[Ir(sacac)(cod)(CH ₃)I]	6	2.832	2.161	2.166	2.153	2.175	2.143	2.076	2.215	2.215	2.215	156.7	156.7	156.1	exp	13j

^a cupf = N-hydroxy-N-nitroso-benzeneamine. ^b neocupf = N-nitroso-N-naphthylhydroxylamine. ^c fctfa = 1-ferrocenyl-4,4-trifluorobutane-1,3-dione. ^d acac = 2,4-pentanedione. ^e sacac = thioacetylacetone.

alkyl-C can be described as distorted octahedral with the bpt⁻ or bpt-NH⁻ ligand, iodide and one of the olefinic bonds to cod in the square plane, see Fig. 4. The deviation from idealized geometry is 7.1–5.8° for angle C_{CH3}-M-I, 8.7–5.4° for angle C_{CH3}-M-A_{cod} and 22.3–18.4° for angle C_{CH3}-M-B_{cod} (see Table 4).

Table 4 summarizes a number of selected geometrical parameters for complexes 5–8, as well as selected rhodium(III) and iridium(III) complexes characterized by X-ray crystallography. The calculated metal-I bond lengths (average 2.9 Å) are slightly longer than the Ir-I bonds in [Ir(sacac)(cod)(CH₃)I]^{13j} and (acac)(cod)(CH₃)I³⁰ (average 2.8 Å) or the Rh-I bonds in [Rh(fctfa)(CO)(CH₃)I(PPh₃)],^{13m} [Rh(cupf)(CO)(CH₃)(I)(PPh₃)]^{13c} and [Rh(neocupf)(CO)(CH₃)(I)(PPh₃)]³⁴ (average 2.7 Å). The M-C_{CH3} bond length (average 2.11 Å), however, is similar to those of the Ir-C_{CH3} bonds in [Ir(sacac)(cod)(CH₃)I]^{13j} and (acac)(cod)(CH₃)I³⁰ (average 2.16 Å) and those of the Rh-C_{CH3} bonds in [Rh(fctfa)(CO)(CH₃)(I)(PPh₃)],^{13m} [Rh(cupf)(CO)(CH₃)(I)(PPh₃)]^{13c} and [Rh(neocupf)(CO)(CH₃)(I)(PPh₃)]³⁴ (average 2.08 Å). The bond lengths between the metal and C_{cod} in the square plane are ca. 0.3 Å shorter than the bonds to the C_{cod} below the plane.

The *cis* addition of CH₃I to the [M(L,L')(cod)] complexes of this study containing a bidentate ligand L,L' with donor atoms L,L' = N,N, is different from what was found for the oxidative addition products of [Ir(sacac)(cod)]^{13j} and [Ir(acac)(cod)]³⁰ containing bidentate ligands L,L' with donor atoms S,S and O,O respectively. In both the oxidative addition products of [Ir(sacac)(cod)] and [Ir(acac)(cod)], the methyl iodide added in a *trans* configuration with substantial steric interaction, as indicated by the large CH₃-Ir-I bond angles (156.1(3) and 156.6(7)°) in these two structures.³¹ However, oxidative addition of SnCl₄ to [M(cod)(μ-Cl)]₂ resulted in a *cis* configuration,³² with a similar coordination sphere (confirmed by X-ray crystallography) around M as was calculated for 5–8. The product of [Ir(cod)(Ph₂PNP(O)Ph₂)] with MeI, (η⁴-cyclo-octa-1,5-diene)-iodo-methyl-(diphenylphosphinylimino(diphenyl)phosphoryl-O,P)-iridium(III),³³ also has the CH₃ and I in a *cis* arrangement with a CH₃-Ir-I bond angle of 82.9°.

Cis methyl iodide addition is also not a novel feature for rhodium(III) complexes and at least two different complexes with *cis* orientated methyl iodide have been isolated and structurally characterized in our laboratories. The I-Rh-CH₃ angles in [Rh(cupf)(CO)(CH₃)(I)(PPh₃)]^{13c} and [Rh(neocupf)(CO)(CH₃)(I)(PPh₃)]³⁴ were determined as 90.8(5) and 91.2(3)°, respectively. Other structurally characterized transition metal complexes having the methyl and iodide in a *cis* arrangement include rac-(di-*t*-butylarsino(di-isopropylphosphino)methane)-(hexafluoroacetylacetonato)-iodido-methyl-rhodium(III),³⁵ iodido-methyl-(η⁵-diphenylphosphinomethyl(dimethyl)silyl-cyclopentadienyl)rhodium(III),³⁶ mer-(2-(diphenylphosphanyl)benzyl)-iodido-methyl-bis(trimethylphosphane)cobalt(I) diethyl ether solvate,³⁷ carbonyl(1,1,1-trifluoro-4-ferrocenyl-2,4-butanedionato-O,O')-iodido-methyl-(triphenylphosphine-P)rhodium(III),^{13m} ((Z)-1-ethyldiazen-1-ium-1,2-diolato)-iodido-methyl-bis(triphenylphosphine)rhodium(I) methanol solvate,³⁸ iodido-methyl-(2-diphenylphosphinophenyl-C,P)-bis(trimethylphosphine)cobalt,³⁹ iodido-methyl-(2,6-bis(1-(2,6-di-isopropylphenylimino)ethyl)pyridine-N,N',N'')rhodium(III) tetrakis(3,5-bis(trifluoromethyl)phenyl)borate dichloromethane solvate,⁴⁰ iodido-methyl-bis(8-methoxynaphthyl-C,O)platinum(IV) deuteriochloroform solvate,⁴¹ *trans*-iodido-methyl-(2,3,5,6-tetrafluoropyrid-4-yl)-bis(triethylphosphine)rhodium(III),⁴² iodido-methyl-(8-dimethylamino-1-naphthyl-C,N)-(8-dimethylamino-1-naphthyl)tin,⁴³ (μ₂-chloranilato)-bis(carbonyl-iodido-methyl-triphenylphosphine-rhodium(III))⁴⁴ and carbonyl-

Table 5 Summary of the kinetic data for the oxidative addition reactions between different[Ir(LL)(cod)] and CH₃I in different solvents and bidentate ligands with different ring sizes at 25 °C.

Complex	Donor atoms	Ring size	$k_f/10^{-2} \text{ L mol}^{-1} \text{ s}^{-1}$	Solvent	Relative permittivity	Ref.
[Ir(macsm)(cod)] ^a	S,N	6	2.84(7)	acetonitrile	37.5	48
[Ir(bpt-NH)(cod)]	N,N	6	1.44(7) 0.092(5)	dichloromethane benzene	8.9 2.3	this study
[Ir(sacac)(cod)] ^b	S,O	6	0.52(3)	acetonitrile	37.5	48
[Ir(tfaa)(cod)] ^c	O,O	6	0.44(2)	acetonitrile	37.5	48
[Ir(sacac)(cod)]	S,O	6	0.34(2)	acetone	20.7	48
[Ir(AnMetha)(cod)] ^d	S,O	5	2.69(6) 0.943(10)	nitromethane acetone	35.87 37.5	13k
[Ir(hpt)(cod)]	S,O	5	2.2(2) 0.693(17)	nitromethane acetone	35.87 37.5	13k
[Ir(bpt)(cod)]	N,N	5	0.35(1)	acetone	20.7	this study
[Ir(cupf)(cod)] ^e	O,O	5	0.217(7)	acetonitrile	37.5	48

^a macsm = methyl(2-methyl-amino-1-cyclopentene-1-dithiocarboxylate).

^b sacac = thioacetylacetone.

^c tfaa = 1,1,1-trifluoro-2,4-pentanedione.

^d AnMetha = 4-methoxy-N-methylbenzothiohydroxamate.

^e cupf = N-hydroxy-N-nitroso-benzeneamine.

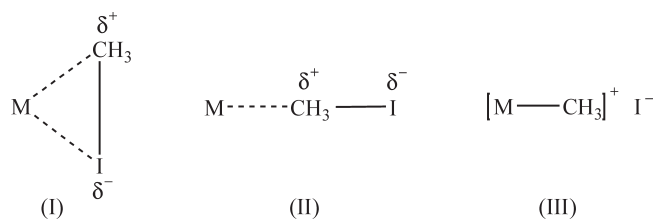
iodido-methyl-(tri-*p*-tolylphosphine)-(quinaldinato-O,N)rhodium diethyl ether solvate.⁴⁵ DFT calculations on the [Rh(β -diketonato)(CO)(PPh₃)₃] complexes with β -diketone = 4,4,4-trifluoro-1-(2-thenoyl)-1,3-propanedione, 1-phenyl-3-(2-thenoyl)-1,3-propanedione, 1,3-di(2-thenoyl)-1,3-propanedione and 1-ferrocenyl-4,4,4-trifluorobutane-1,3-dione, in agreement with experimental observations, also found the *cis* addition product of CH₃I to these square planar rhodium(I) complexes to be the most stable.⁴⁶

It is clear from Fig. 4 that one of the centroids of the cod ligand is forced out of the N,N plane and is replaced by the iodine, possibly due to the steric interaction between the methyl group and the cod ligand. This steric interaction is clearly evident in the *trans*-oriented products where both the methyl group and the iodide are forced from an ideal *trans* orientation (180 °) to angles smaller than 160 °.

3.2. Oxidative Addition Kinetics

The kinetic results showed very simple second-order kinetics indicating the straightforward formation of the M(III) alkyl product from the M(I) cod complex. All the results showed a linear dependence on CH₃I concentration and all the intercepts were calculated to be zero within experimental error. A summary of the kinetic data is given in Table 1 and an example is presented in Fig. 1. The oxidative addition for both the bpt complexes was followed in acetone while the bpt-NH complexes were followed in both benzene and DCM as solvents. From the results in Table 1 it appears that the iridium-bpt complex reacts about 17 times faster than the corresponding rhodium complex, while the opposite was observed for the bpt-NH complexes, where the rhodium complex underwent oxidative addition approximately twice as fast as the corresponding iridium complex. The latter observation is contrary to the general tendency for oxidative addition reactions, predicting that iridium complexes undergo oxidative addition faster than the corresponding rhodium complexes.⁴⁷ For both complexes the rate of oxidative addition was slower in the non-polar solvent. The slower reactions in the non-polar solvents are not surprising if the oxidative addition step involves charge separation in the transition state, such as postulated for a concerted three-centred (I) or two-step

S_N2 mechanism (II). The latter should produce an ionic intermediate (III) which will be facilitated by polar solvents such as DCM and this intermediate is converted to the coordinatively saturated *cis* or *trans* oxidative addition product in a fast consecutive step.



The activation entropy values are all relatively large and negative, indicating an associative interaction with bond formation in the transition state for the metal complexes that were studied.

Table 5 presents a summary of the oxidative addition reactions by different iridium cyclo-octadiene complexes that were studied. Since the ring sizes as well as the L,L' donor atoms of the bidentate rings coordinated to the iridium cyclo-octadiene complexes differ, a direct comparison of the available data is difficult. The current study, however, contributes to the small library of available data of oxidative addition reactions to iridium cyclo-octadiene complexes.

4. Conclusion

Three new triazolato complexes, two for iridium(I) and one for rhodium(I), were successfully synthesized and characterized by elemental analysis, IR and ¹H NMR spectroscopy. The oxidative addition products were successfully isolated and characterized by ¹H NMR, IR and elemental analysis. Although no crystals suitable for X-ray crystallography could be obtained, the geometry of bpt-NH⁻ complexes, as well as the final products, were successfully identified with DFT calculations. These calculations indicated that the bpt-NH⁻ ligand forms a six-membered chelate ring with the metal centres while the oxidative addition products have a *cis* methyl iodide orientation. The kinetic study indicated slower oxidative addition reactions in non-polar solvents for both metals, suggesting charge separation during the formation of the transition state. Large negative values for the activation entropies indicate associative interaction in the transition state.

Supplementary Material

A summary of the optimized Cartesian coordinates of the studied molecules is provided in the supplementary material.

Acknowledgements

Financial assistance by the South African National Research Foundation and the Central Research Fund of the University of the Free State is gratefully acknowledged.

References and Notes

- 1 J.H. Jones, *Platinum Metal Rev.*, 2000, **44**, 94–105.
- 2 G.J. Sunley and D.J. Watson, *Catalysis Today*, 2000, **58**, 293–307.
- 3 J. Plotkin and L. Song, www.ics.com/Articles/2003/04/04/193199, accessed 29 September 2008.
- 4 A. Haynes, P.M. Maitlis, G.E. Morris, G.J. Sunley, H. Adams, P.W. Badger, C.M. Bowers, B. Cook, P.I.P. Elliot, T. Ghaffar, H. Green, T.R. Griffin, M. Payne, J.-M. Pearson, M.J. Taylor, P.W. Vickers and R.J. Watt, *J. Am. Chem. Soc.*, 2004, **126**, 2847–2861.
- 5 T.W. Dekleva and D. Foster, *Advan. Catal.*, 1986, **34**, 81–130.
- 6 P.M. Maitlis, A. Hayes, G.J. Sunley and M.J. Howard, *J. Chem. Soc., Dalton Trans.*, 1996, 2187–2196.
- 7 A. Hayes, B.E. Mann, D.J. Gulliver, G.E. Morris and P.M. Maitlis, *J. Am. Chem. Soc.*, 1991, **113**, 8567–8569.
- 8 (a) J. Rankin, A.D. Poole, A.C. Benyei and D.J. Cole-Hamilton, *Chem. Commun.*, 1997, 1835–1836; (b) C.M. Thomas, A. Neels, H. Stoekli-Evans and G. Süß-Fink, *Eur. J. Inorg. Chem.*, 2001, 3005–3008; (c) J.A. Gaunt, V.C. Hayens, S.K. Spitzmesser, A.J.P. White and D.J. Williams, *Organometallics*, 2004, **23**, 1015–1023.
- 9 P. Das, P. Chutia and D.K. Dutta, *Chem. Lett.*, 2002, 766–767.
- 10 P. Das, M. Sharma, N. Kumari, D. Konwar and D.K. Dutta, *Appl. Organomet. Chem.*, 2002, **16**, 302–306.
- 11 N. Kumari, M. Sharma, P. Chutia and D.K. Dutta, *J. Mol. Catal.*, 2004, **222**, 53–58.
- 12 B.J. Sarmah, B.J. Borah, B. Deb and D.K. Dutta, *J. Mol. Catal.*, 2008, **289**, 95–99.
- 13 (a) S.S. Basson, J.G. Leipoldt and J.T. Nel, *Inorg. Chim. Acta*, 1984, **86**, 167–172; (b) S.S. Basson, J.G. Leipoldt, A. Roodt, J.A. Venter and T.J. van der Walt, *Inorg. Chim. Acta*, 1986, **119**, 35–38; (c) S.S. Basson, J.G. Leipoldt, A. Roodt and J.A. Venter, *Inorg. Chim. Acta*, 1987, **128**, 31–37; (d) J.G. Leipoldt, S.S. Basson and L.J. Botha, *Inorg. Chim. Acta*, 1990, **168**, 215–220; (e) J.G. Leipoldt, E.C. Steynberg and R. van Eldik, *Inorg. Chem.*, 1987, **26**, 3068–3070; (f) G.J. van Zyl, G.J. Lamprecht, J.G. Leipoldt and T.W. Swaddle, *Inorg. Chim. Acta*, 1988, **143**, 223–227; (g) J.G. Leipoldt, G.J. Lamprecht and G.J. van Zyl, *Inorg. Chim. Acta*, 1985, **96**, L31–L34; (h) D.M.C. Smit, S.S. Basson, A. Roodt and E.C. Steynberg, *Rhodium Express*, 1994, **7–8**, 12–16; (i) Y.M. Terblans, S.S. Basson, W. Purcell and G.J. Lamprecht, *Acta Cryst.*, 1995, **C51**, 1748–1750; (j) P. Ebenebe, S.S. Basson and W. Purcell, *Rhodium Express*, 1996, **16**, 11–16; (k) M. Theron, E. Grobbelaar, W. Purcell and S.S. Basson, *Inorg. Chim. Acta*, 2005, **358**, 2457–2463; (l) E. Grobbelaar, W. Purcell and S.S. Basson, *Inorg. Chim. Acta*, 2006, **359**, 3800–3860; (m) J. Conradie, G.J. Lamprecht, A. Roodt and J.C. Swarts, *Polyhedron* 2007, **23**, 5075–5087; (n) M.M. Conradie and J. Conradie, *Inorg. Chim. Acta*, 2008, **361**, 2285–2295; (o) J. Conradie and J.C. Swarts, *Organometallics* 2009, **28**, 1018–1026.
- 14 D.E. Graham, G.J. Lamprecht, I.M. Potgieter, A. Roodt and J.G. Leipoldt, *Transition Met. Chem.*, 1991, **16**, 193–199.
- 15 G.J.J. Steyn, A. Roodt, I. Poletaeva and Y.S. Varsavsky, *J. Organomet. Chem.*, 1997, **536**, 197–205.
- 16 L.J. Botha, S.S. Basson and J.G. Leipoldt, *Inorg. Chim. Acta*, 1987, **126**, 25–28.
- 17 L.J. Damoense, *Fundamental Aspects of Selected Rhodium Complexes in Homogeneous Catalytic Acetic Acid Production*, Ph.D. thesis, University of the Free State, Bloemfontein, South Africa, 2001.
- 18 D.D. Perrin and W.L.F. Armarego, *Purification of Laboratory Chemicals*, 3rd edn., Pergamon Press, Oxford, UK, 1988.
- 19 *Scientist*, Version 2, MicroMath Scientific Software, St. Louis, MO, USA, 2004.
- 20 J.F. Geldard and F. Lions, *J. Org. Chem.*, 1965, **30**, 318–319.
- 21 S.A. Bezman, P.H. Bird, A.R. Fraser and J.A. Osborn, *Inorg. Chem.*, 1980, **19**, 3755–3763.
- 22 G. Giordano and R.H. Crabtree, *Inorg. Synthesis*, 1990, **28**, 88–90.
- 23 (a) N.C. Handy and A.J. Cohen, *Mol. Phys.*, 2001, **99**, 403–412; (b) C. Lee, W. Yang and R.G. Parr, *Phys. Rev. B*, 1988, **37**, 785–789.
- 24 J. Stephens, F.J. Devlin, C.F. Chabalowski and M.J. Frisch, *J. Phys. Chem.*, 1994, **98**, 11623–11627.
- 25 (a) E. van Lenthe, A.E. Ehlers and E.J. Baerends, *J. Chem. Phys.*, 1999, **110**, 8943–8953; (b) E. van Lenthe, E.J. Baerends and J.G. Snijders, *J. Chem. Phys.*, 1993, **99**, 4597–4610; (c) E. van Lenthe, E.J. Baerends and J.G. Snijders, *J. Chem. Phys.*, 1994, **101**, 9783–9792; (d) E. van Lenthe, J.G. Snijders and E.J. Baerends, *J. Chem. Phys.*, 1996, **105**, 6505–6516; (e) E. van Lenthe, R. van Leeuwen, E.J. Baerends and J.G. Snijders, *Int. J. Quantum Chem.*, 1996, **57**, 281–293.
- 26 G.T. Velde, F.M. Bickelhaupt, E.J. Baerends, C.F. Guerra, S.J.A. Van Gisbergen, J.G. Snijders and T. Ziegler, *J. Comput. Chem.*, 2001, **22**, 931–967.
- 27 M.P. Garcia, J.A. Manero, L.A. Oro, M.C. Aperda, F.H. Cano, J.G. Haasnoot, R. Prins and J. Reedijk, *Inorg. Chim. Acta*, 1986, **122**, 235–241.
- 28 H.M. Burke, J.F. Gallagher, M.T. Indelli and J.G. Vos, *Inorg. Chim. Acta*, 2004, **357**, 2989–3000.
- 29 (a) J. Conradie, G.J. Lamprecht, S. Otto and J.C. Swarts, *Inorg. Chim. Acta*, 2002, **328**, 191–203; (b) M.M. Conradie and J. Conradie, *Inorg. Chim. Acta*, 2008, **361**, 208–218.
- 30 S.S. Basson, J.G. Leipoldt, W. Purcell and J.B. Schoeman, *Acta Cryst.*, 1989, **C45**, 2000–2001.
- 31 DFT calculations at the same level of theory as for this study indicated that the *cis*1 and the *trans* oxidative addition products of [Ir(sacac)(cod)] are equienergetic. The same result is obtained for [Ir(acac)(cod)]. The *cis* addition found for the metal-triazolato complexes of this study is thus real and not a consequence of the computational method used.
- 32 (a) J. Choudhury, S. Podder and S. Roy, *J. Am. Chem. Soc.*, 2005, **128**, 6162–6163; (b) J. Choudhury, D. K. Kumar and S. Roy, *J. Organomet. Chem.*, 2007, **392**, 5614–5620.
- 33 A.M.Z. Slawin, M.B. Smith and J.D. Woollins, *J. Chem. Soc., Dalton Trans.*, 1996, 1283–1293.
- 34 J.A. Venter, *Structural and Kinetic Study of Rhodium Complexes of N-aryl-N-nitrosodihydroxyamines and Related Complexes*, Ph.D. thesis, University of the Free State, Bloemfontein, South Africa, 2006.
- 35 H. Werner, U. Schmidt, B. Weberndorfer and C.D. Brandt, *Z. Anorg. Allgem. Chem.*, 2002, **628**, 2383–2394.
- 36 L. Lefort, T.W. Crane, M.D. Farwell, D.M. Baruch, J.A. Kaeuper, R.J. Lachicotte and W.D. Jones, *Organometallics*, 1998, **17**, 3889–3899.
- 37 H.-F. Klein, R. Beck, U. Florke and H.-J. Haupt, *Eur. J. Inorg. Chem.*, 2003, 853–862.
- 38 N. Arulsamy, D.S. Bohle and B. Doletski, *Helv. Chim. Acta*, 2001, **84**, 3281–3288.
- 39 H.-F. Klein, S. Schneider, M. He, U. Floerke and H.-J. Haupt, *Eur. J. Inorg. Chem.*, 2000, 2295–2301.
- 40 E.L. Dias, M. Brookhart and P.S. White, *Organometallics*, 2000, **19**, 4995–5004.
- 41 E. Wehman, G. van Koten, C.T. Knaap, H. Oссор, M. Pfeffer and A.L. Spek, *Inorg. Chem.*, 1988, **27**, 4409–4417.
- 42 D. Noveski, T. Braun, B. Neumann, A. Stammeler and H.-G. Stammeler, *Dalton Trans.*, 2004, 4106–4111.
- 43 J.T.B.H. Jastrzebski, P.A. van der Schaaf, J. Boersma, G. van Koten, D.J.A. De Ridder and D. Heijdenrijk, *Organometallics*, 1992, **11**, 1521–1526.
- 44 A. Elduque, Y. Garces, L.A. Oro, M.T. Pinillos, A. Tiripicchio and F. Uguzzoli, *J. Chem. Soc., Dalton Trans.*, 1996, 2155–2158.
- 45 M. Cano, J.V. Heras, M.A. Lobo, E. Pinilla and M.A. Monge, *Polyhedron*, 1992, **11**, 2679–2690.
- 46 (a) M.M. Conradie and J. Conradie, *Inorg. Chim. Acta*, 2009, **362**, 519–530; (b) M.M. Conradie and J. Conradie, *S. Afr. J. Chem.*, 2008, **61**, 102–111.
- 47 R.S. Nyholm and K. Vrieze, *J. Chem. Soc.*, 1965, 5337–5340.
- 48 Y.M. Terblans, *Oxidative Addition Kinetics of Iridium(I) Cyclo-octadiene Complexes with Iodomethane* (translated), M.Sc. thesis, University of the Free State, Bloemfontein, South Africa, 1993.